

FOLIO

TA7

C6

CER-68-69-27

Cap. 2

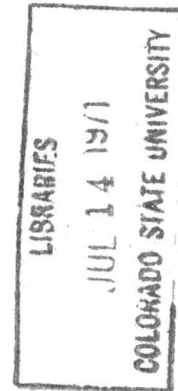
LIBRARY  
COLORADO STATE UNIVERSITY  
FORT COLLINS, COLORADO

RESEARCH AND DEVELOPMENT TECHNIQUE FOR ESTIMATING  
AIRFLOW AND DIFFUSION PARAMETERS IN CONNECTION WITH  
THE ATMOSPHERIC WATER RESOURCES PROGRAM

February 1969

by

J. E. Cermak  
L. O. Grant  
M. M. Orgill



Research and Development Technique for Estimating  
Airflow and Diffusion Parameters in Connection with  
the Atmospheric Water Resources Program

Interim Report

February 1969

Prepared by

J. E. Cermak  
L. O. Grant  
M. M. Orgill

Period July 1, 1968 to December 31, 1968  
Atmospheric Water Resources Research  
Bureau of Reclamation  
Contract No. 14-06-D-6455

Fluid Dynamics and Diffusion Laboratory  
College of Engineering  
Colorado State University  
Fort Collins, Colorado

## Abstract

Preliminary experiments on transport and dispersion over a 1:9,600 scale model of the Eagle River Valley and topography surrounding Climax, Colorado were obtained in the Colorado State University meteorological wind tunnel. Geometric, dynamic and thermal similarity are considered, primarily, for neutral stability flows. Similarity for transport and dispersion is considered briefly.

Pilot balloon flights, a super pressure balloon flight and ice nuclei concentrations taken during a field trip in the Climax area are presented.

Table of Contents

Page

A. Introduction	
1. General statement of the problem . . . . .	1
2. General objectives . . . . .	2
B. Laboratory study	
1. Topographic models . . . . .	3
2. Flow similarity	
a. Assumptions . . . . .	4
b. Thermal similarity . . . . .	4
c. Geometric similarity and boundary conditions . . . . .	5
d. Dynamic and kinematic similarity . . . . .	5
3. Similarity requirements for transport and dispersion . . . . .	6
4. Experimental equipment	
a. Wind tunnel . . . . .	8
b. Instrumentation . . . . .	8
c. Visualization techniques . . . . .	10
5. Experimental results	
a. Air flow with neutral stability . . . . .	11
b. Air flow with stable stratification . . . . .	13
C. Field work	
1. Field project - 16-20 December 1968. . . . .	13
2. Instrumentation and data . . . . .	14
3. Field results	
a. Pilot balloon flights . . . . .	15
b. Superpressure balloon flights . . . . .	15
c. Ice nuclei concentrations . . . . .	16

	<u>Page</u>
D. Numerical simulation . . . . .	16
E. Future work . . . . .	17
F. Appendix . . . . .	18

References

Figures

## List of Figures

- Figure 1 Topography of experimental area with generator locations
- Figure 2 Eagle River Valley topographic model
- Figure 3 Experimental apparatus for dispersion measurements
- Figure 4 Variation of static pressure over topographic model at free stream level (107 cm above tunnel floor)
- Figure 5 Velocity profiles with upstream roughness and without roughness on model
- Figure 6 Velocity profiles with screens, vortex generators, ridge and roughness on model
- Figure 7 Vertical profile of turbulent intensity near silver iodide generator site (Redcliff)
- Figure 8 Vertical displacement of concentration plume downwind from Redcliff source.
- Figure 9 Concentration plume downwind from Redcliff source (lateral)
- Figure 10 Velocity profiles from pilot balloon flights at Camp Hale
- Figure 11 The horizontal (A) and vertical (B) trajectories of a super-pressure balloon over the Arkansas River Valley during southwest flow. 19 December 1968
- Figure 12 Change in ice nuclei concentration at Climax after seeding at upwind ground sites during light and moderate snowfall

## List of Symbols

$\theta$	Potential temperature
$\beta$	Coefficient of stability $\frac{1}{\theta} \frac{\partial \theta}{\partial z}$
T	Temperature
$\tau_0$	Surface shear stress
$\bar{U}$	Mean velocity
$\rho$	Density of air
$C_D$	Drag coefficient
L	Length
t	Time
U	Typical velocity scale or local velocity
$\vec{r}$	Vector distance downwind of source (x,y,z)
Q	Source strength; time rate of material emission from a continuous point source
$\chi$	Concentration at a point (x,y,z) at time t
$\bar{\chi}$	Average concentration
$V_s$	Effluent ejection speed
$\rho_s$	Mass density (or temperature) of effluent
$C_o$	Rate of coagulation
$\Lambda$	Rate of interception with aerosols (washout, etc.)
$V_{gr}$	Sedimentation velocity (gravity)
R	Rate of chemical, radioactive and radiative transformation
E	Electrification effects
$\vec{H}$	Topographic profile (x,y,z)
$\epsilon$	Height of surface irregularities (trees, etc.)
$\vec{V}$	Vector wind velocity at a given height

$\vec{V}_g$	Gradient or free stream velocity
$\frac{\partial \vec{v}}{\partial z}$	Directional and speed wind shear
$K_{ij}$	Coefficients of eddy diffusivity
I	Rate of interaction with land, snow and water surfaces (storage and reflection).
$\delta$	Boundary layer thickness
$u'$	Fluctuating velocity component in the longitudinal direction (downwind)
E	D.C. output voltage
f	Coriolis parameter $2\Omega \sin \phi$ where $\Omega$ - Angular velocity of the earth $\phi$ - Latitude
$U_L$	Local free stream

## A. Introduction

### 1. General statement of the problem

One of the revolutionary discoveries of cloud physics took place during 1947 when Vonnegut discovered the great efficiency of silver iodide as an ice-crystal nucleus. Since then introduction of silver iodide into cloud structures has become the major technique used in cloud modification studies.

Silver iodide acts in a cloud in essentially the same manner in which the natural freezing-nuclei in the atmosphere act. It is, therefore, only necessary to distribute silver iodide smoke through the air-mass in which clouds are forming in order for it to influence their development and stability.

If a supercooled cloud is seeded with silver iodide, the ice crystals produced grow at the expense of the cloud droplets and fall with increasing rapidity, emerging from the cloud base as snow flakes or raindrops. However, since the liquid water content of the cloud is also decreased it is possible (depending on the seeding rate) for overseeding to occur resulting in cloud dissipation.

Studies have indicated that orographic cloud systems in which systematic condensation is caused by geographical features are most suitable for seeding. However, the obtaining of optimal distribution of seeding material in orographic cloud systems presents a complex theoretical and operational problem.

A pertinent discussion of the optimization seeding problem for orographic clouds is well described by McDonald (1958):

From the stand point of optimizing cloud seeding, one wishes to be able to predict what flux of nuclei should be released at the generator

site in order to insure a specified concentration at a given level within clouds at a roughly given distance. An error of much more than one order of magnitude in concentration may, on existing theory, spell the difference between seeding success and failure, yet such a precision places demands on turbulence theory that cannot at present be met, above all under conditions of airflow over orographic barriers of complex form. Since seeding of orographic clouds holds, in many ways, better promise than seeding of any other cloud type, this difficulty is not a trivial one.

Several techniques such as, aircraft, ground generators, balloons, rockets, anti-aircraft guns and natural rising air currents have been utilized in an attempt to place the seeding material within the clouds. For storm situations, ground based generators are usually utilized in mountainous terrain due to economical and safety factors.

The realization of optimal distribution of seeding material in cloud systems presents a complex operational and logistic problem, particularly, if a field sampling program is required to provide adequate information on dispersion mechanisms. An alternative method may consist of conducting transport and dispersion experiments with a laboratory facility for the initial input data then utilize numerical models and field project data to verify or correct the laboratory results. Such a technique would appear valuable for beginning weather modification projects where information regarding dispersion processes may not be well known.

## 2. General objectives

The following are the general objectives for the proposed research:

- a. Determine the full capability for simulating flow over mountain barriers.
- b. Investigate the feasibility of simulating dispersion characteristics and transport of particulate material such as silver iodide with a wind tunnel model.

- c. Evaluate the potential value of wind tunnel simulation for weather modification operations in various types of orographic terrain.

## B. Laboratory study

### 1. Topographic models

The first topographic model of this study simulates the Eagle River Valley area and topography surrounding Climax, Colorado, Fig. 1. The direction of the freestream wind is approximately  $320^{\circ}$  or northwest. The scale of the model is 1:9,600 which was governed by the width of the existing tunnels and the vertical thickness of the building material (expanded polystyrene bead board). Construction details were given in earlier progress reports. Figure 2 shows the model during construction and during experimental periods in the tunnel.

A particular problem of importance is attempting to model the roughness features such as forests, rocks, etc.. After a futile search for something better it was decided to model the roughness features by use of gravel. A grain size of 1.168 mm and less was utilized for valley and timberline roughness while a grain size of approximately 1.68 mm was utilized for forest areas. This was essentially a scale down of prototype roughness features. The grains of gravel were cemented on the model by using velvet latex paint.

Measurements of height above the model were usually taken from the lowest point which for the prototype is 7,800 ft (2379 m) above sea level.

## 2. Flow similarity

### a. Assumptions

In the case of flow around or over obstacles such as mountains, geometrical, kinematical, dynamical, and thermal similarity should be achieved. However, due to laboratory limitations certain atmospheric processes of secondary importance compared to orographic effects are not included in laboratory simulation. These are:

- 1) Coriolis acceleration,
- 2) compressibility of the air,
- 3) condensation, evaporation, radiation, and
- 4) unsteady state of prototype winds (including diurnal variations).

Wind tunnel results when compared with field data should assist in determining the importance of these various variables on transport and dispersion in the lower atmosphere.

### b. Thermal similarity

For the Climax area many cloud seeding operations are scheduled for storm situations. An examination of the past available radiosonde data for Chalk Mt. shows that many storm situations with northwest flow exhibit near neutral stability lapse rates up to at least 500 MB. Neutral stability implies that  $\frac{\partial \theta}{\partial z} = 0$  or  $\beta = 0$ .

In the wind tunnel the temperature distribution is usually isothermal or  $\frac{\partial T}{\partial z} = 0$ . However, it can be shown that this stability condition is equivalent to neutral stability since potential temperature in the atmosphere corresponds closely to density (temperature) in an incompressible fluid.

Wind tunnel results for this period are nearly all done under neutral stability conditions. Modeling different stability conditions than neutral will be attempted during the next period of work.

c. Geometric similarity and boundary conditions

The lower boundary condition is provided by the topographic model. Similarity of the approach flow requires that the upstream shear flow have a vertical distribution of mean velocity similar to the prototype (atmosphere). The best approximation is to develop a turbulent boundary layer which is several times thicker than the height of the topographic features. This is usually accomplished by a long test section, roughening the approach surface or other artificial devices such as screens, grids, etc.

d. Dynamic and kinematic similarity

Typical values of the Reynolds number for prototype and model are  $10^8$  and  $10^5$ , respectively. If the air is in neutral stability and the flow is aerodynamically rough Reynolds number similarity is not required as long as the value of the Reynolds number in the tunnel exceeds  $10^4$ . In such cases the mean-flow patterns are independent of the Reynolds number or viscosity (Garrison and Cermak 1968).

This type of similarity implies that the surface shear stress is

$$\tau_{o_m} = \frac{1}{2} C_{D_m} \rho_m \bar{U}_m^2 \quad \text{model}$$

$$\tau_{o_p} = \frac{1}{2} C_{D_p} \rho_p \bar{U}_p^2 \quad \text{prototype}$$

or that

$$\rho_m \bar{U}_m^2 = \rho_p \bar{U}_p^2$$

if for high Reynolds number flow it is assumed that  $C_{D_m} \sim C_{D_p}$ .

From the above relation

$$\bar{U}_m = \sqrt{\frac{\rho_p}{\rho_m}} \bar{U}_p$$

and using typical tunnel and prototype densities

$$\bar{U}_m = 0.943 \bar{U}_p \quad \rho_m = 0.977 \text{ Kg/m}^3$$

$$\rho_p = 0.864 \text{ Kg/m}^3$$

which shows that for high Reynolds number flow the mean velocities in the tunnel and prototype atmosphere should be approximately the same.

It is important to note how the time-scales of the wind fluctuations are related for model and prototype. If the time-scale of the model is  $t_m$  and that of the real flow  $t_p$ , then we have

$$t_m = \frac{L_m}{L_p} \frac{U_p}{U_m} t_p$$

If  $t_p = 1 \text{ hour}$ ,  $U_p = U_m$  and using our scale ratio 1:9,600

$$t_m = 0.375 \text{ sec}$$

### 3. Similarity requirements for transport and dispersion

The concentration  $\chi$  in a particulate plume over mountainous terrain is affected by numerous variable, e.g.,

$$\chi(\vec{r}, t) = f(Q, V_s, \rho_s, C_o, \Lambda, V_{gr}, R, E, I, \vec{H}, \epsilon, \delta, \vec{V}, \vec{V}_g, \rho, f, \beta, \frac{\partial \vec{v}}{\partial z}, K_{ij})$$

where the number and selection of variables follows from suggestions given by Monin (1959).  $Q, V_s, \rho_s$  are parameters depending on the source characteristics.  $C_o, \Lambda, V_{gr}, R, E, I$  are physical variables depleting the particulate material in transit.  $\vec{H}$  and  $\epsilon$  describe the topographic terrain.  $\vec{V}$  and  $\vec{V}_g$  represent the transport by mean motions (synoptic, mesoscale, etc.).

$\beta, \frac{\partial \vec{v}}{\partial z}, K_{ij}$  are parameters which influence turbulent mixing.

Owing to the number of variables involved, modeling of dispersion in atmospheric motions can lead to so many scale factors as to make the problem extremely difficult if not impossible to manage. Therefore, a selection must be made as to which variables are significant for a particular case, or, more realistically it must be determined which types of atmospheric motions are capable of being modeled.

For a wind-tunnel model of our scale length it is very difficult to scale or simulate all aspects of the source characteristics and properties of the particulate material. However, details of the source characteristics are rapidly lost as mixing takes place downstream and exact simulation is not essential. We have utilized helium as a tracer material because a method of detection is available. Other tracers such as radioactive krypton may be better to avoid buoyancy effects. Neglecting these aspects the concentration is given by

$$\chi(\vec{r}, t) = f(\vec{H}, \epsilon, \vec{V}, \vec{V}_g, \delta, \rho, f, \beta, \frac{\partial \vec{v}}{\partial z}, K_{ij}) .$$

However, if geometric similarity is assumed and  $f$  and  $\beta$  are neglected (neutral stability) then the important variables are  $\vec{V}, \vec{V}_g, \delta, \frac{\partial \vec{v}}{\partial z}$  and  $K_{ij}$ .

For this experimental period we have attempted to model the first four parameters  $\vec{V}, \vec{V}_g, \delta, \frac{\partial \vec{v}}{\partial z}$  on the basis of limited field data available at the time. However, since the laboratory results were obtained some additional field data have been collected and these results will be presented in section C3. The variable  $K_{ij}$  was also simulated to some extent since it depends primarily upon the surface characteristics and the conditioning of the boundary layer upstream from the model. Lack of similiarity exists only insofar as  $K_{ij}$  depends upon additional meso- or large-scale effects.

#### 4. Experimental equipment

##### a. Wind tunnel

All the experimental work was accomplished in the Colorado State University low-speed recirculating wind tunnel. The tunnel is driven by a 75 h.p. DC motor and contains a 9.2 meter test section length which is 1.8 x 1.8 meters in cross section. A complete description of the wind tunnel is given in a brochure - Fluid Mechanics Program (1966).

##### b. Instrumentation

The mean velocity distributions for high velocity neutral flows were measured utilizing pitot tubes, an electronic differential pressure transducer (Transonic Equibar Type 120) and a X-Y plotter (Moseley Type 135).

Mean velocity distributions at low ambient speed during stable stability conditions have been obtained by a visualization technique (Sanders 1967). A nichrome wire  $3.81 \times 10^{-3}$  cm in diameter and about 30 cm in length is coated with low viscosity oil which is vaporized by passage of an electrical pulse through the wire. The resultant line source of smoke is then photographed. The distance traveled by a point in the smoke trace downwind from the vertical wire is proportional to the local mean wind speed.

The fluctuating velocity component in the longitudinal direction  $\overline{u'^2}$  was measured with a single wire probe. The sensor was a tungsten wire which had a diameter of  $5.08 \times 10^{-4}$  cm. The hot-wire probe was operated by a constant temperature hot-wire anemometer and the output was

received by a Bruel and Kjaer rms meter. The rms of the turbulent velocity fluctuations were obtained from the relation

$$\sqrt{\overline{u'^2}} = \sqrt{\overline{e^2}} / \frac{\partial E}{\partial U}$$

where the relation between  $E$  and  $U$  was obtained from calibration and Kings law,

$$E^2 = A + BU^{1/2} .$$

The dispersion measurements consisted of measuring helium concentration over the topographic model with a split sector mass spectrometer contained in a Veeco helium leak detector (Model MS-12AB). The source and sampling system utilized is schematically illustrated in Fig. 3. The flow-rate of helium to the source on the model surface was controlled by a pressure regulator at a helium bottle outlet and by a sensitive flow meter. The source exit velocity was maintained at 7-8 m/sec throughout the experiments. The helium was emitted from a brass tubing of 0.159 cm diameter. The source locations were placed on the model as close as possible to the actual prototype silver iodide generator locations.

The sampling probe was a brass tubing of 0.3 cm diameter and was mounted on a traversing carriage whose horizontal and vertical position was controlled remotely from outside the tunnel. The gas sample was continuously drawn into the sampling probe by a small vacuum pump at a constant velocity of 25 cm/sec.

The helium and other components in the air flow are drawn into the split sector mass spectrometer where the neutral atoms and molecules are converted to positively charged ions by a regulated beam of electrons. Upon, formation, these ions encounter electrostatic fields established

within the ion source which accelerate the ions out of the ion source in a well-defined, mono-energetic beam. A magnetic analyzer serves to separate the helium ions from the remainder of the ion beam, and to pass these ions on to the detector. Once the current of helium ions has been separated from all the other species of ions an electron multiplier converts the helium ion current to a measurable output which is amplified and converted to a visible meter deflection on the portable leak-indicator meter. Visual readings from one to two minutes were taken and recorded.

Since a closed circuit wind tunnel was utilized an ambient concentration of helium built up with time. Therefore, several ambient concentration measurements were taken with each profile. The relative concentration was obtained by subtracting the corresponding ambient concentration from the absolute concentration. All data presented in the figures are relative concentrations.

Calibration was obtained with helium-nitrogen mixtures of known helium concentration (0.2 and 0.01). Calibration was obtained before and after each experimental run.

#### c. Visualization techniques

Two methods were utilized in obtaining qualitative information on dispersion and surface wind patterns over the model. The first technique used chemical smoke and was employed both in neutral and stable flows. An electric pump forces two chemical vapors,  $\text{NH}_4\text{OH}$  and  $\text{HCl}$  through two separate tubings which were placed in the tunnel upstream from the model. Mixing of the chemical vapors in the tunnel produces a resultant plume of  $\text{NH}_4\text{Cl}$  smoke which is highly visible, especially in stable flow.

A small portion of liquid  $\text{TiCl}_4$  placed in the tunnel also provided a good smoke source but is rather toxic.

For high velocity neutral flows, a small pivoting directional vane was utilized for depicting the spatial surface flow directions. The directional vane was constructed of fine glass tubing approximately 2 cm in length. A piece of nylon thread (1.5 cm) was tied and cemented around the center of the glass tubing. A size 8 sewing needle was inserted into the glass tubing and mounted vertically on the model. The directional vanes are very sensitive to surface flows down to 2 m/s. With proper lighting and camera setting the directional vanes show clearly in motion pictures and slides.

## 5. Experimental results

### a. Air flow with neutral stability

Figure 3 shows the experimental apparatus for neutral stability flows. The free stream velocity in these cases was  $V_g = 12 \text{ m/s}$ . However, due to the blockage of the model in the tunnel the free stream velocity increases locally over the model. Figure 4 shows the static pressure distribution in the free stream region.

A thick boundary layer is required in dispersion experiments therefore it was necessary to modify the velocity profiles. Figure 5 shows the velocity distribution and boundary layer thickness over the topographic model when the only artificial roughness was a bed of small gravel several meters upstream. To thicken the boundary layer, several methods using screens, fences, etc. were tried until the configuration in Fig. 3 was chosen. The artificial devices used were: 1) one 5 cm, one 10 cm and three 20 cm

screens, 2) a vortex generator (McVehil 1967) consisting of 16 delta wings. Each generator consisted of a 30 cm semi-span of a delta wing with a 45 degree sweep angle. They protruded vertically from the floor and were arranged at alternate incidence angles of 10 degrees to the oncoming flow. Mean spacing of the downwind edges was 5 cm. A 45° ridge was placed horizontally across the tunnel upstream from the model and represents an actual extension of the topographic features of the area.

The utilization of these devices gave a very thick boundary layer as attested by Fig. 6. Since the boundary layer over the mountains is not well known we are not sure what exact height of boundary layer thickness is required, however, a boundary layer between 40 to 50 cm appears adequate.

Figure 7 shows one profile of the turbulent intensity in the longitudinal direction (downwind). In addition, visual observations of chemical smoke indicated that the model flow was very turbulent. The high intensity of turbulence was due in part to the phenomenon of separation. Separation occurred on the leeside of the upstream ridge and in several valleys oriented perpendicular to the flow. A large separation zone associated with the upstream ridge had a pronounced effect on the initial direction of the lower level flow and dispersion.

Concentration measurements of helium were obtained from two source locations, Minturn and Redcliff. Only the data for the Redcliff source are shown since there was some question on the reliability of the Minturn results. Figures 8 and 9 show the concentration profiles of helium in parts per million over the model terrain.

Since helium is lighter than air a slight buoyancy effect is present especially when the helium first leaves the source probe. This is the

reason for the slight jump in the concentration plume near the source.

It is encouraging to note that the concentration plume is fairly realistic and with improvements in techniques based upon these experiments it should be possible to obtain reliable estimates of the lateral and vertical extent of the plume as well as the downwind concentration distribution.

b. Airflow with stable stratification

Some preliminary experiments were conducted utilizing 500 lbs of solid carbon dioxide upstream from the model in order to achieve a stable (inversion) flow condition. This laboratory arrangement provides low flow speeds (15 cm/sec) that are required for satisfying other thermal similarity requirements.

The smoke wire was utilized in obtaining velocity profiles and chemical smoke ( $\text{NH}_4\text{Cl}$ ) sources provided visual observation of dispersion. These experiments along with the neutral stability results assisted in determining where new sites for field instruments should be located (see C 2).

C. Field work

1. Field project - 16-20 December 1968

Field project coordinators, L. Grant and L. Hjermstad organized the annual field trip to the Climax area. Various field groups (see Appendix) participated in obtaining several types of field observations.

The synoptic weather situation proved favorable at times, however, snow, cold temperatures, and changing wind conditions prevented completion of all objectives. Wind directions were southwest early in the week, changing to northwest for one day, then changing to south-southwest in the latter part of the week.

## 2. Instrumentation and data

Radiosonde flights were taken at three sites during this period:

a) Chalk Mountain, b) fish hatchery and c) Camp Hale. Pilot balloon flights were taken at five different sites. One superpressure balloon flight was obtained during south-southwest flow in the Arkansas River Valley west of Leadville. Counts of ice crystals were obtained by a Bigg-Warner expansion type ice nuclei counter on the summit of Chalk Mountain and at the High Altitude Observatory (H.A.O.).

Five new field sites for weather equipment were established or modified during this time. Laboratory experiments assisted in locating these field sites. Locations and equipment are as follows:

a. North end of Camp Hale.

50 foot tower with wind direction vane and anemometer;

Instrument shelters with microbarograph and hygro-thermograph.

b. North end of Chicago Ridge at 11,000 feet elevation.

Same instruments as above.

c. Summit of Tennessee Pass.

Same instruments but wind direction vane and anemometer to be installed on a 125 foot tower.

d. Upper Fork of Eagle River below H.A.O.

Same instruments as a. and b.

e. Summit of Chalk Mountain.

Modification of instruments and a 80 foot tower will be erected so equipment for measuring turbulent components of the wind can be installed.

These weather station sites and others, in conjunction with radiosonde data,

will assist in showing the temperature and humidity variations with elevation as well as the surface wind variations.

### 3. Field results

#### a. Pilot Balloon flights

Single theodolite pilot balloon flights were made in the Eagle River Valley at the north end of Camp Hale. Figure 10 shows three of these flights up to 5054 meters (16,580 ft.) during general northwest wind directions. We hope to obtain similar data for other locations in the valley to get a better picture of the velocity distribution during northwest flow.

#### b. Superpressure balloon flights

A superpressure balloon is made of a rigid material so that its volume is essentially constant with superpressure. The balloon will seek a density level where the weight of air displaced by it is exactly equal to the weight of the balloon, helium and all attachments. If the balloon is displaced above or below that density level, it becomes negatively or positively buoyant and seeks to return to its original level. Thus, it is in stable equilibrium on a particular density surface. The only way the balloon will be displaced from the equilibrium density level is by vertical air currents or by a change of mass or volume of the balloon itself. If the balloon is designed so that its mass can not change and if it is free of leaks, it can be expected to remain at its equilibrium density level indefinitely except for temporary displacements due to vertical air movements (Booker 1965).

Superpressure balloon flights were planned both for southwest flow and northwest flow but the latter was cancelled due to poor visibility. The site for the flight during southwest flow was along an east-west road from Malta to the fish hatchery. A double theodolite technique was utilized for tracking the balloon since radar equipment was not available.

A pillow shaped balloon was weighted to fly at approximately 500 ft (~152 meters) and released from a location (~100 yds) just south of the eastern theodolite. Figure 11 shows the resultant horizontal and vertical

trajectories of the balloon as determined from a computer program. Maximum vertical velocities of  $\pm 1$  m/s or more were observed and the horizontal speed varied from 2.5 to 13.3 m/s.

c. Ice nuclei concentrations

Figure 12 shows the concentrations of ice nuclei during the seeding event December 17-18, 1968. Three seeding generators were operated during this period. Wind directions and speeds at Chalk Mt. and H.A.O. are plotted during this period as well as the duration and intensity of snowfall. Ice nuclei counts were observed both at Chalk Mt. and H.A.O.

Figure 12 indicates that seeding materials are being observed at ground stations in the Climax target area when released 11 to 16 miles upwind. The rapid increases in ice nuclei concentrations some 3 to 4 hours after the generators at Redcliff and Minturn were turned on, provides reasonable evidence that some portion of the seeding material is reaching the Climax site.

Ice nuclei concentration fluctuations appear to be related, in part, to wind direction changes. Large increases in ice nuclei counts (17th 1800 - 1930 p.m. and 18th 0100 - 0200 a.m.) correspond with wind shifts to northwesterly directions while decreases occur with wind shifts to the north and northeasterly directions.

Future dispersion experiments should assist in defining the plume more accurately than presently known.

D. Numerical simulation

Although not directly funded by this project, numerical simulation of dispersion and transport over mountainous terrain has been in progress for

several months. M. Fosberg (Forest Service) assisted in setting up the essentials of the numerical program. The program obtains a two-dimensional flow over an irregular boundary by solving for a stream function which has been modified by boundary and stability conditions. The stream function field and a continuous point source are then incorporated into the diffusion equation in order to compute the concentration downwind. This computer model will allow any desired two-dimensional mountain profile to be generated. Unfortunately, computational problems have prevented us from getting good results to date. Evaluation of these problems is underway at the present time.

#### E. Future work

##### 1. Model construction

The next topographic model to be constructed will simulate the southwest wind direction in the Climax area. This model may be a little more difficult to construct since it includes Mt. Elbert and Mt. Massive areas. Scale and construction methods will be essentially the same as for the other models.

##### 2. Laboratory experiments

###### a. Eagle River model (northwest flow)

Additional experiments will attempt to improve similarity between model and prototype in regard to velocity profiles, stability characteristics, turbulence, and dispersion. Dispersion measurements with stable stability flow may be attempted if problems regarding source material are solved adequately.

b. Elk Mt. model (southwest flow)

Interest has been expressed in attempting to model convective regimes over irregular topography. Since Elk Mt. is relative simple in relief such experiments may be attempted with this model.

Dispersion experiments will be conducted either during this period or the next.

3. Field work and numerical simulation

If a favorable northwest wind synoptic pattern appears between now and April another short field trip will be planned and executed.

During the remainder of this project period work will be directed toward a reasonable plan to conduct field dispersion experiments for the next project period (1969 - 1970). Meteorological tracers, detection equipment, and cost will be investigated in order to get a better understanding of such a program.

The numerical simulation work will proceed as indicated in the report.

F. Appendix

The following personnel were associated with the research project during the period under review:

1. Professional staff	<u>Project responsibility</u>
<u>Name</u>	
J. E. Cermak	Principal investigator
L. O. Grant	Coordinates field program with laboratory experiments
M. M. Orgill	Supervised laboratory experiments, and analysis of data; assisted in obtaining field data; numerical simulation

<u>Name</u>	<u>Project responsibility</u>
J. A. Garrison	Assisted with laboratory experiments
L. Hjermsstad	Directed field data collection program
G. Wooldridge	Assisted in obtaining field data
C. Chappell	Assisted in obtaining field data
W. Kamm	Computer programming
2. Graduate research assistants and student help	
D. Nambudiripad	Data reduction
S. Brown	Field work
R. Potter, III	Construction of models
W. Tully	Construction of models
3. Technical assistance	
B. Johnson	Construction of smoke wire circuit
J. Buckley	Construction of smoke wire
4. Western Scientific Service, Inc. (sub-contractor)	
J. Jones	Field work
P. Hayes	Field work
D. Cobb	Field work
J. Price	Field work
5. Other Assistance (not funded by project)	
G. Hsi	Assisted with laboratory experiments
D. Kesic	Assisted with laboratory experiments

## References

- College of Engineering, 1966: Fluid Mechanics Program. Fluid Dynamics and Diffusion Laboratory, Colorado State University, pp 36.
- Booker, Ray D. and Lynn W. Cooper, 1965: Superpressure balloons for weather research. Journal of Applied Meteorology, Vol. 4, No. 1, pp 122-129.
- Garrison, J. A. and J. E. Cermak, 1968: San Bruno Mountain wind investigation - A wind-tunnel model study. Fluid Dynamics and Diffusion Laboratory Report CER 67-68JEC-JAG58, Colorado State University. 89 pp.
- McDonald, J. E., 1958: Physics of cloud modification. Advances in Geophysics, Vol. 5, pp. 278-280.
- McVehil, G. E., G. R. Ludwig, and T. R. Sundaram, 1967:  
On the feasibility of modeling small scale atmospheric motions. CAL Report No. ZB-2328-P-1 Cornell Aeronautical Laboratory, Inc. 152 pp.
- Monin, A. S., 1959: General survey of atmospheric diffusion, Advances in Geophysics. Vol. 6, pp. 29-40.
- Sanders, Curren I., and J. F. Thompson, Jr., 1967: An evaluation of the smoke-wire technique for measuring velocities in air. USAAVLABS Technical Report 67-29, Mississippi State University. 43 pp.



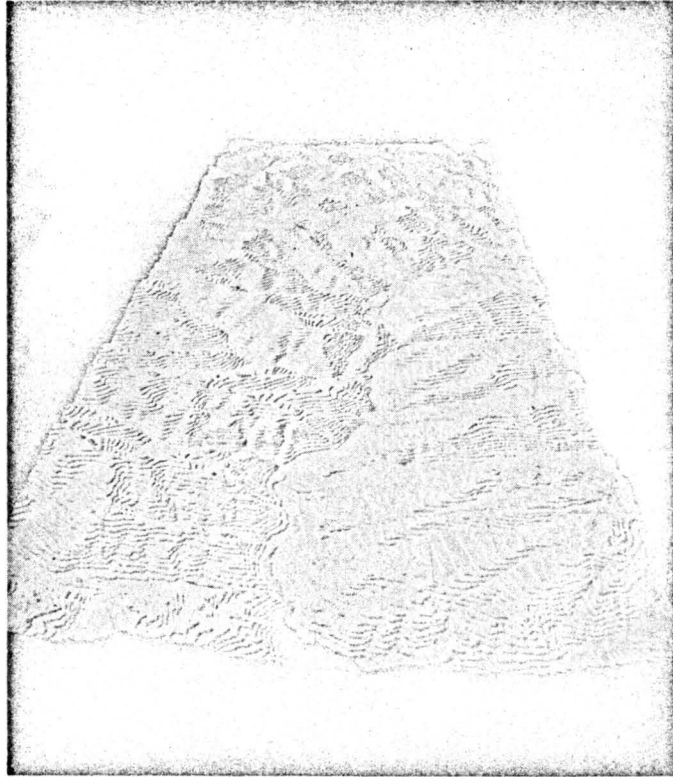


Figure 2 Eagle River Valley topographic model

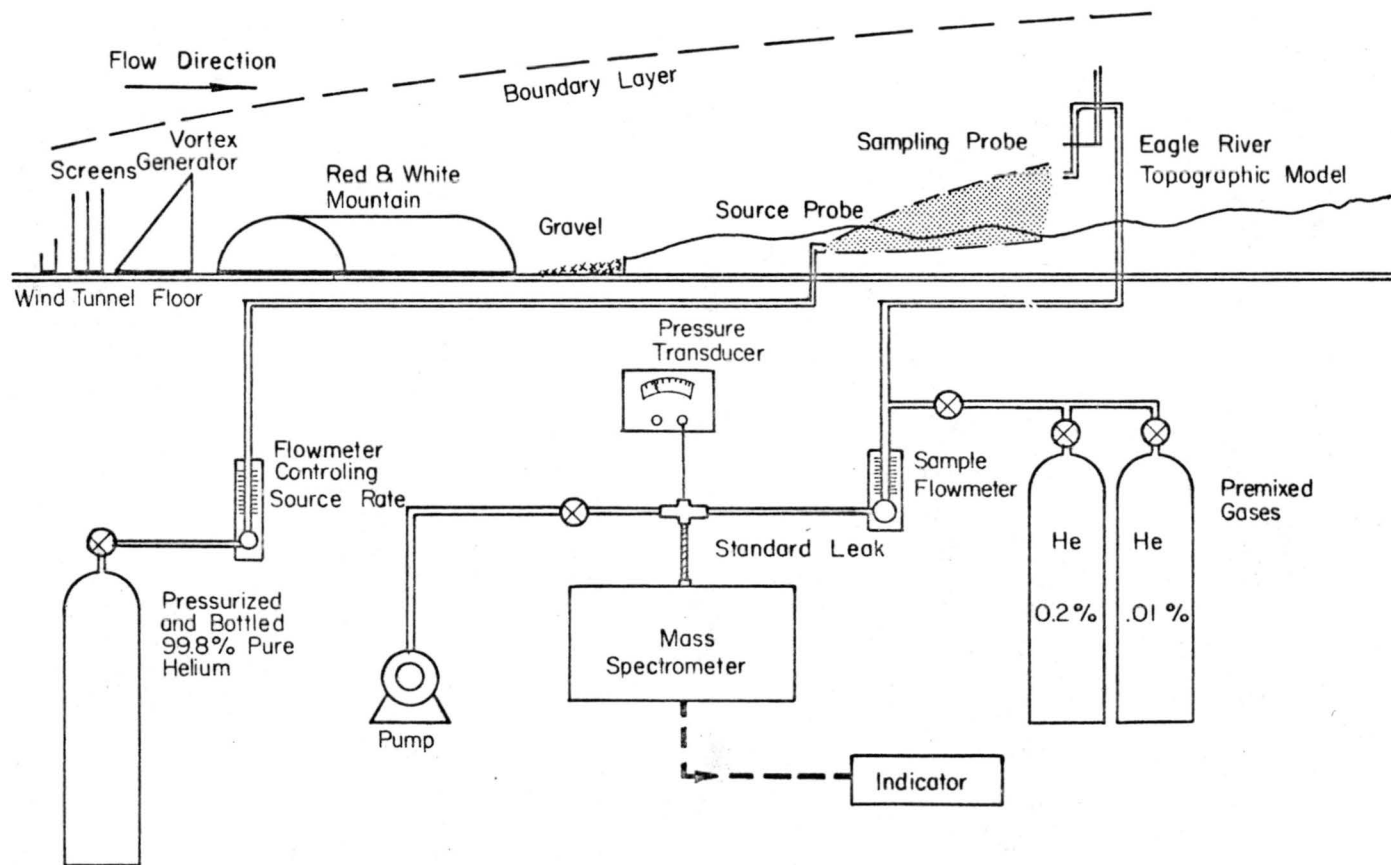


Figure.3 Experimental Apparatus for Dispersion Measurements

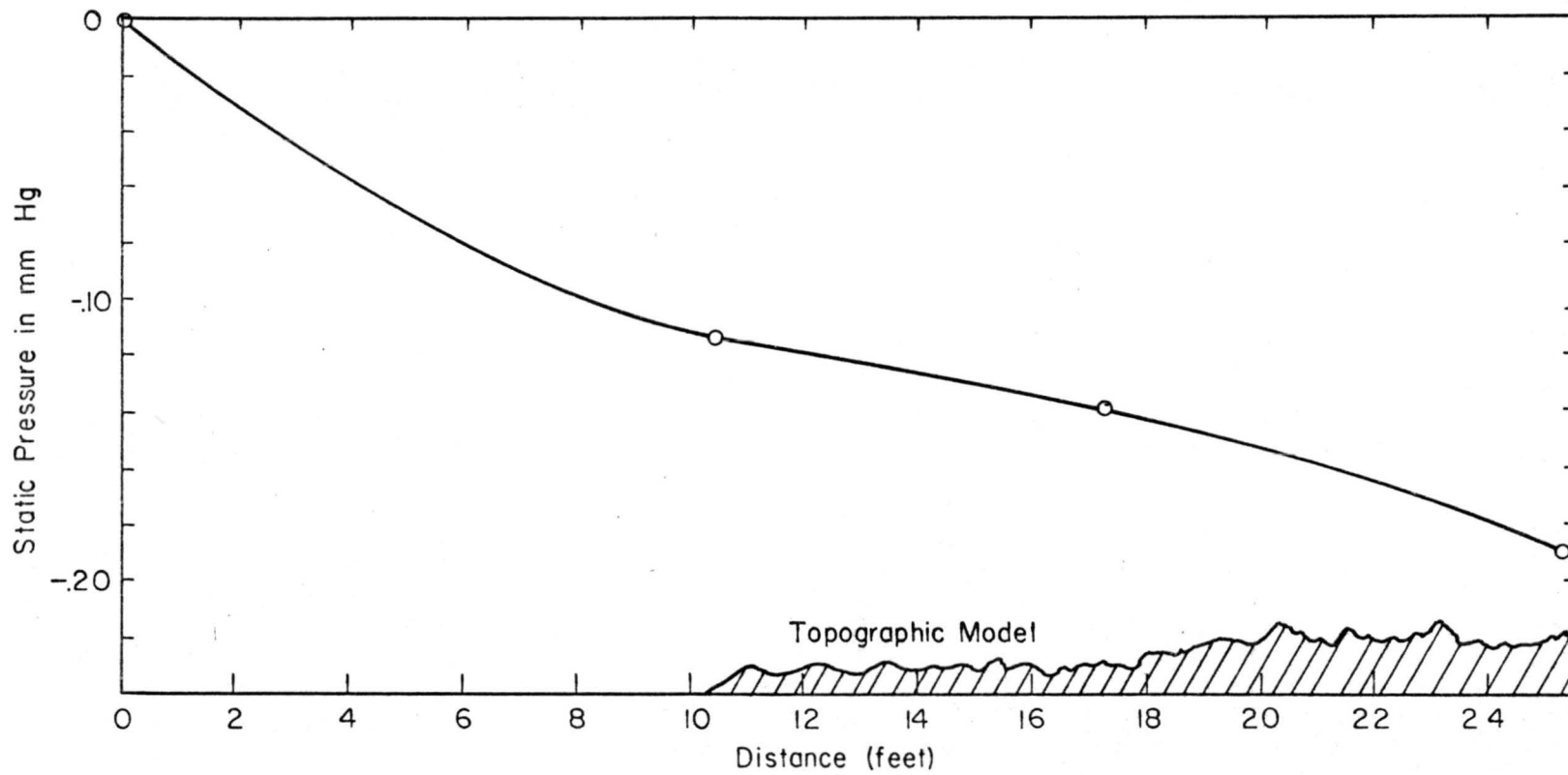


FIGURE 4— Variation of Static Pressure over Topographic Model at Free Stream Level.  
(107cm Above Tunnel Floor)

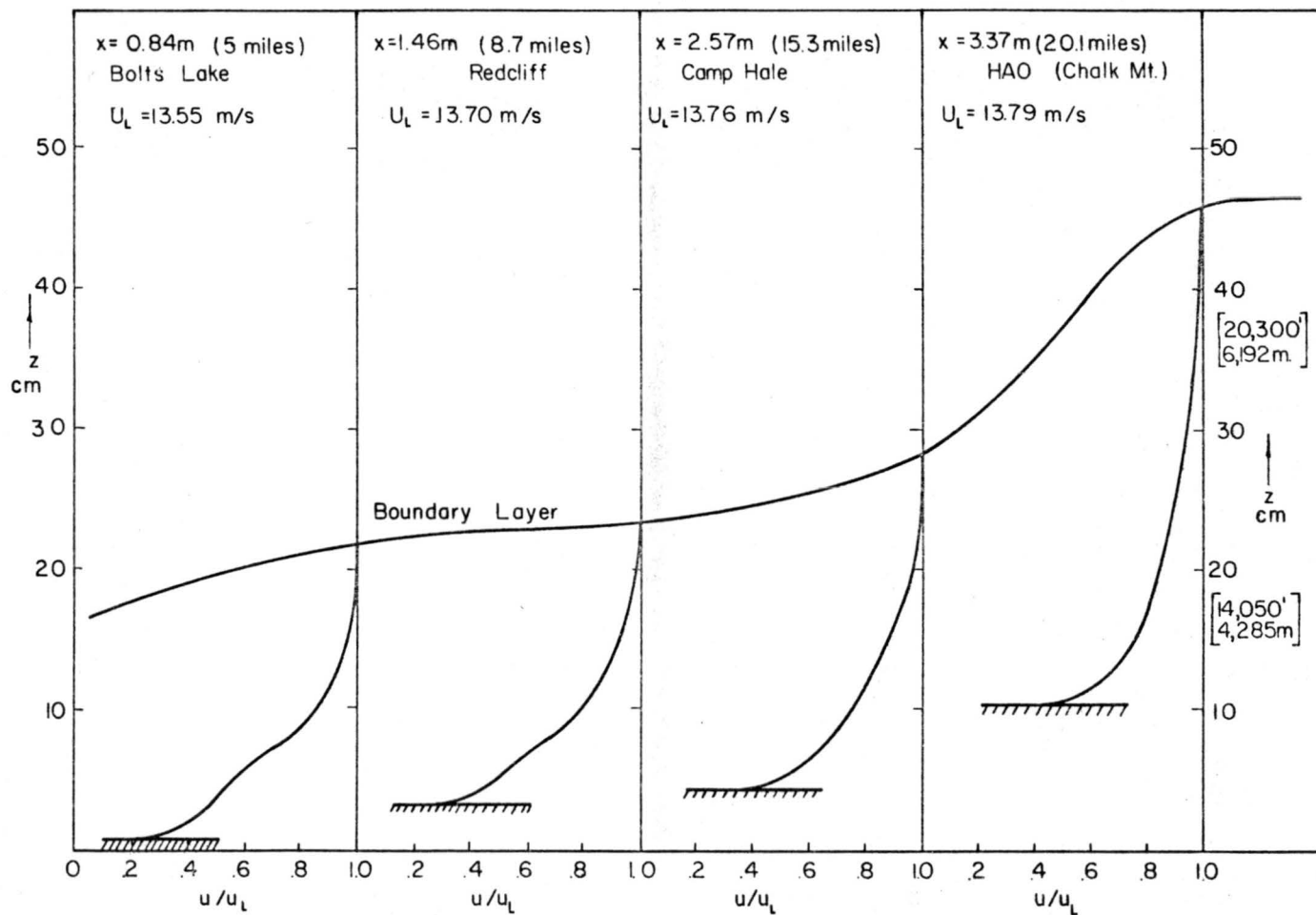


Figure 5 Velocity profiles with upstream roughness and without roughness on model.

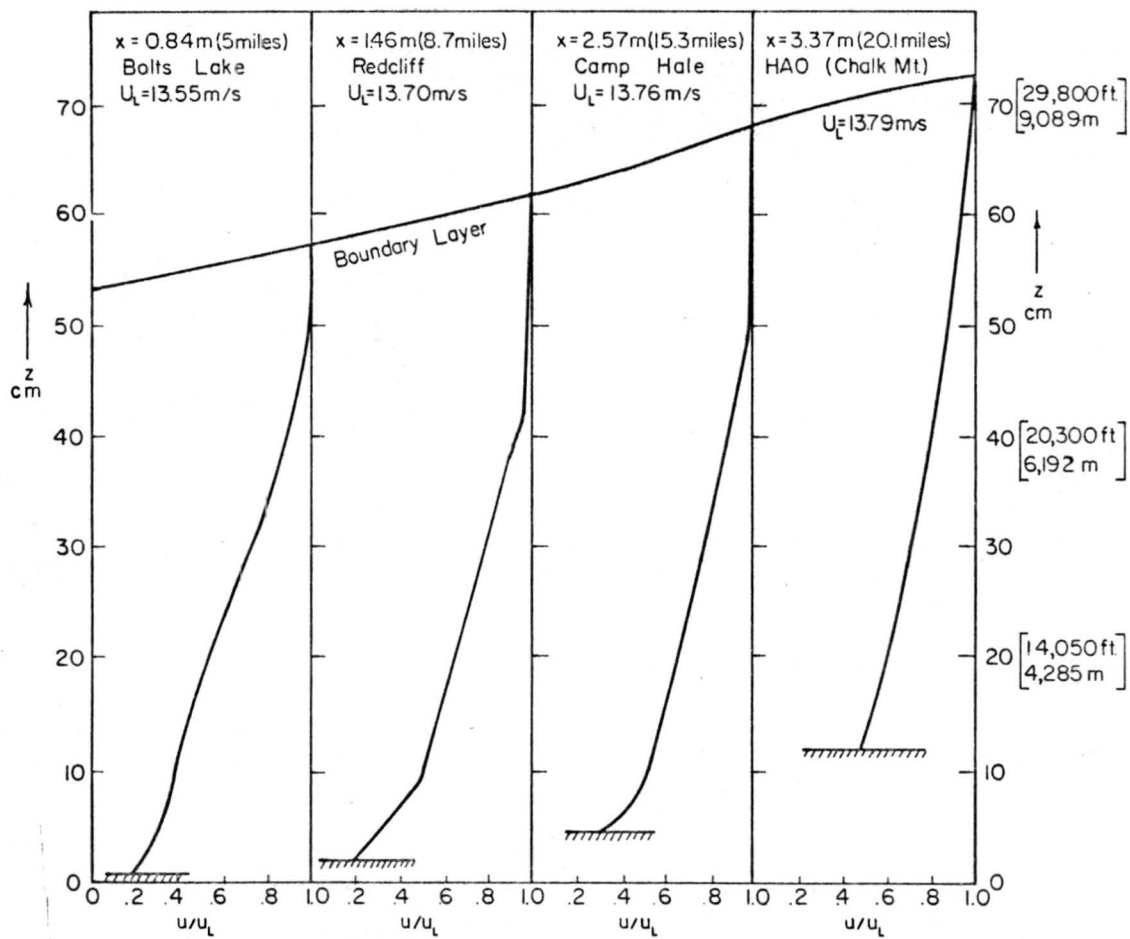


FIGURE 6- Velocity Profiles with Screens, Vortex Generator, Ridges and Roughness on Model.

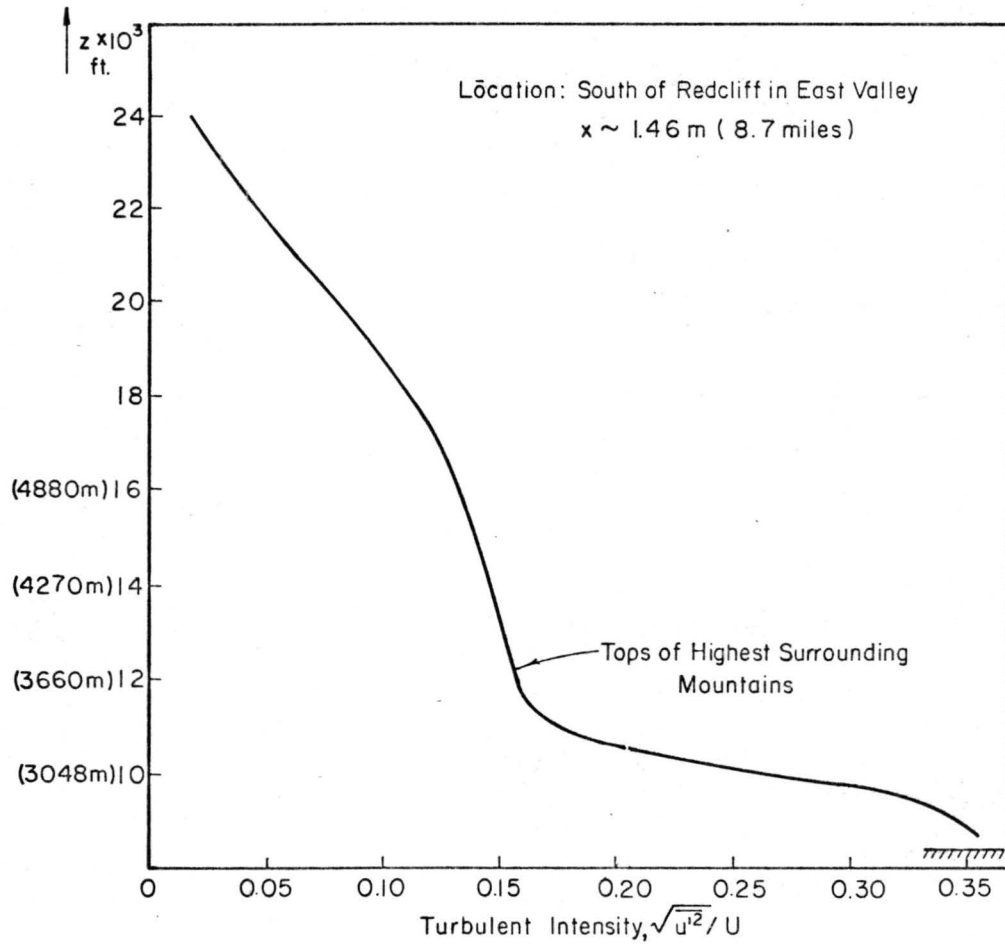


FIGURE-7 Vertical Profile of Turbulent Intensity Near Silver Iodide Generator Site (Redcliff).

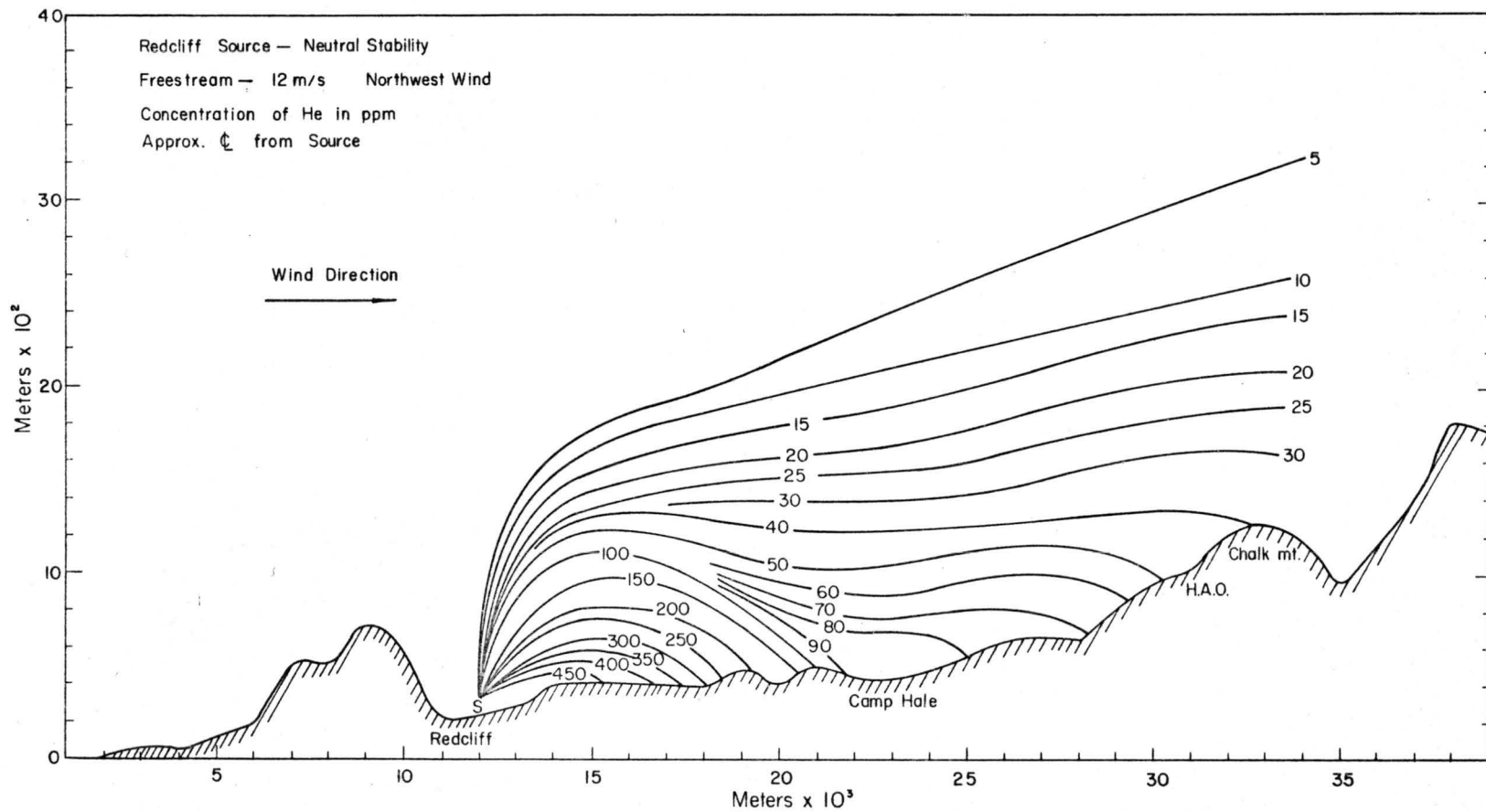


FIGURE 8 Vertical Displacement of Concentration Plume Downwind from Redcliff Source.

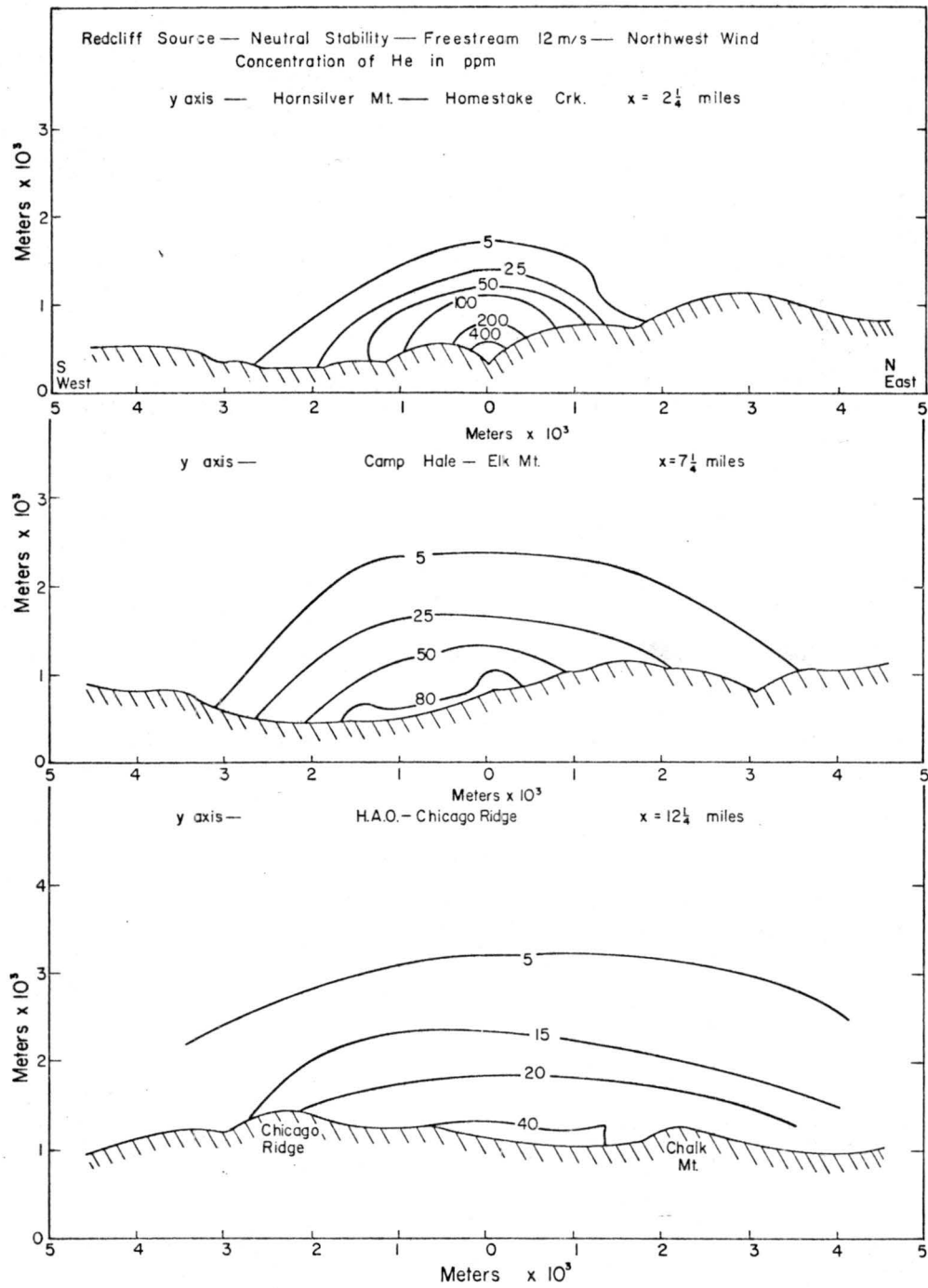


FIGURE 9— Concentration Plume Downwind from Redcliff Source.

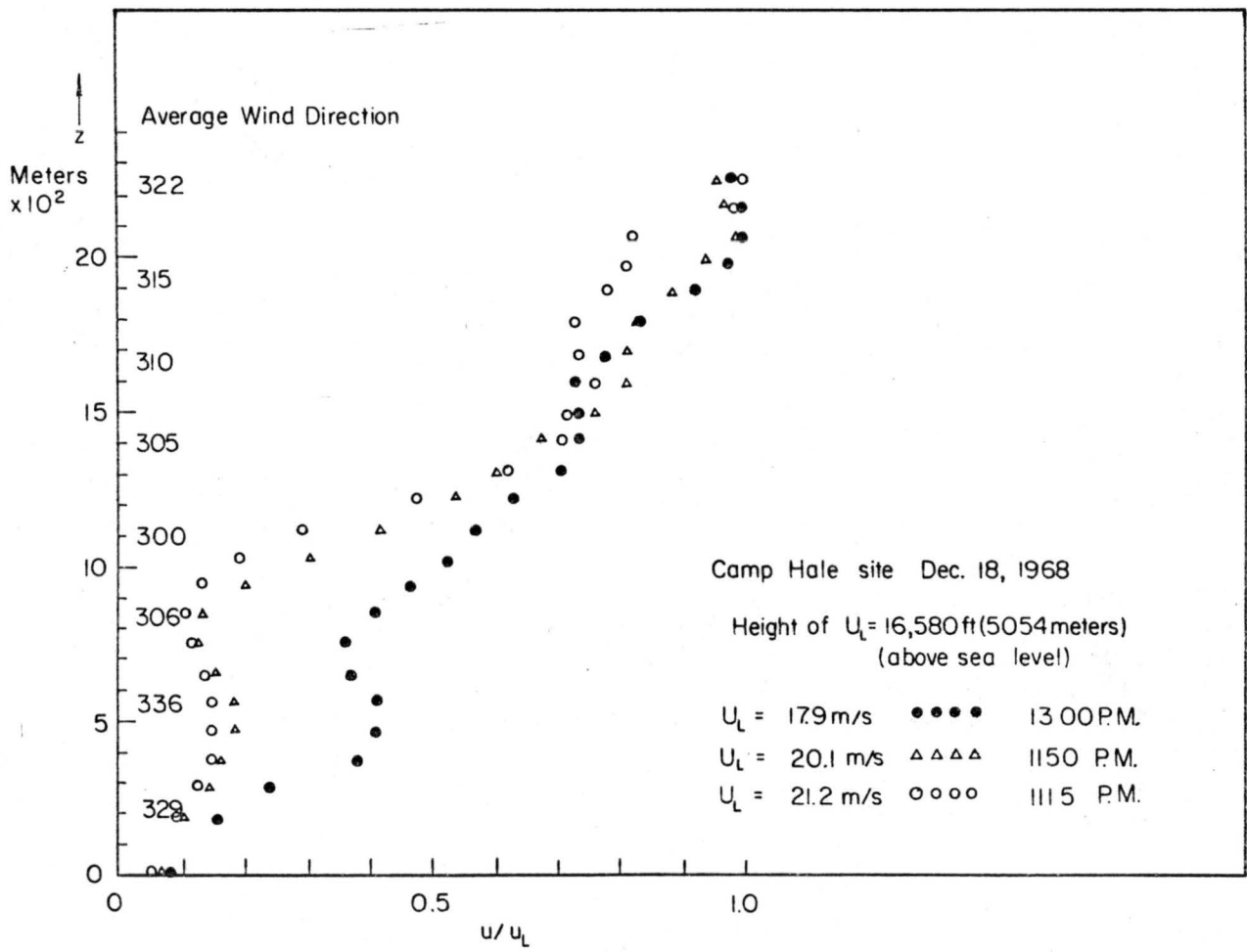


FIGURE 10 Velocity Profiles from Pilot Balloon Flights at Camp Hale.

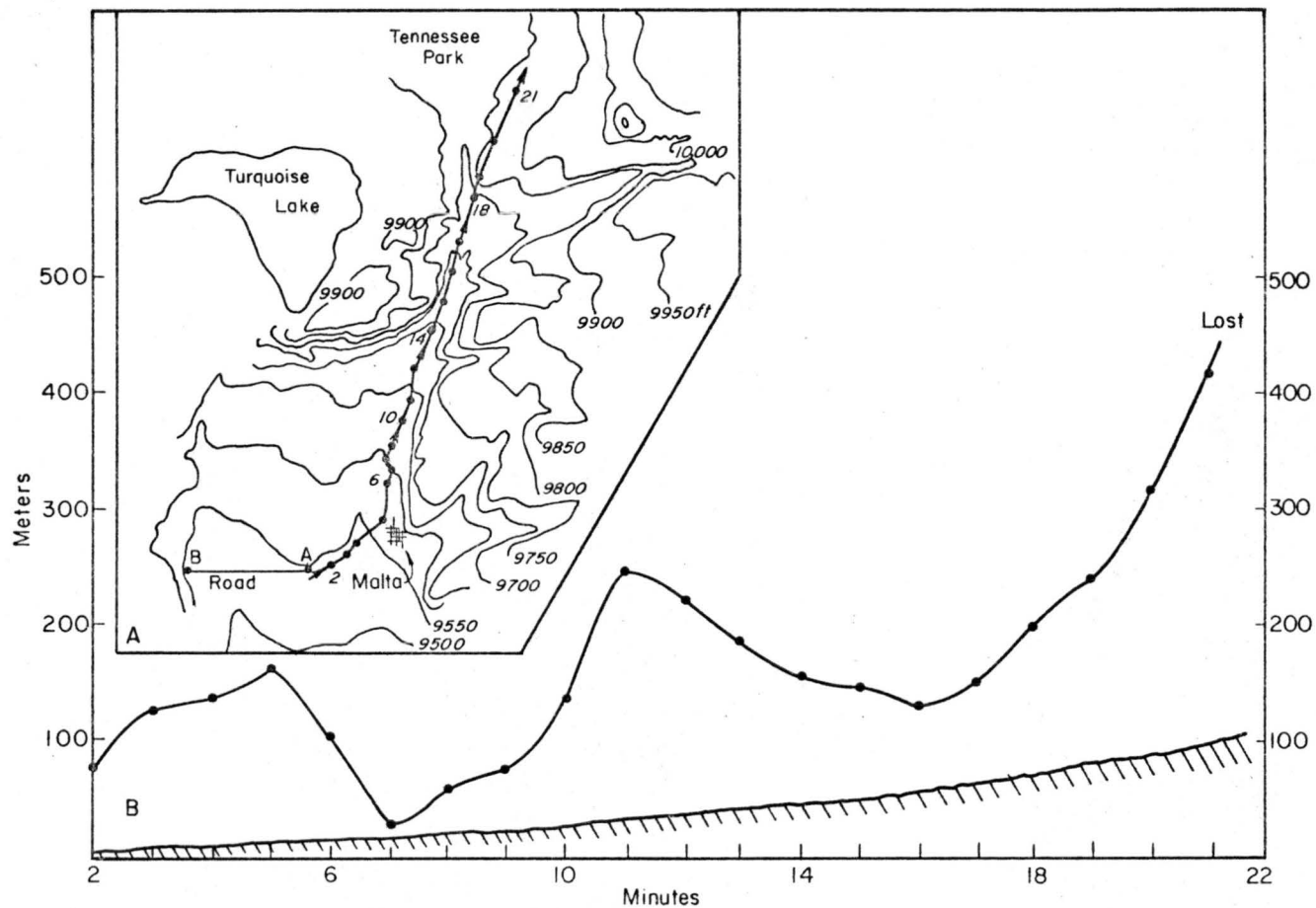


Fig. 11. The Horizontal (A) and Vertical (B) Trajectories of a Superpressure Balloon Over the Arkansas River Valley During Southwest Flow 19 Dec. 1968

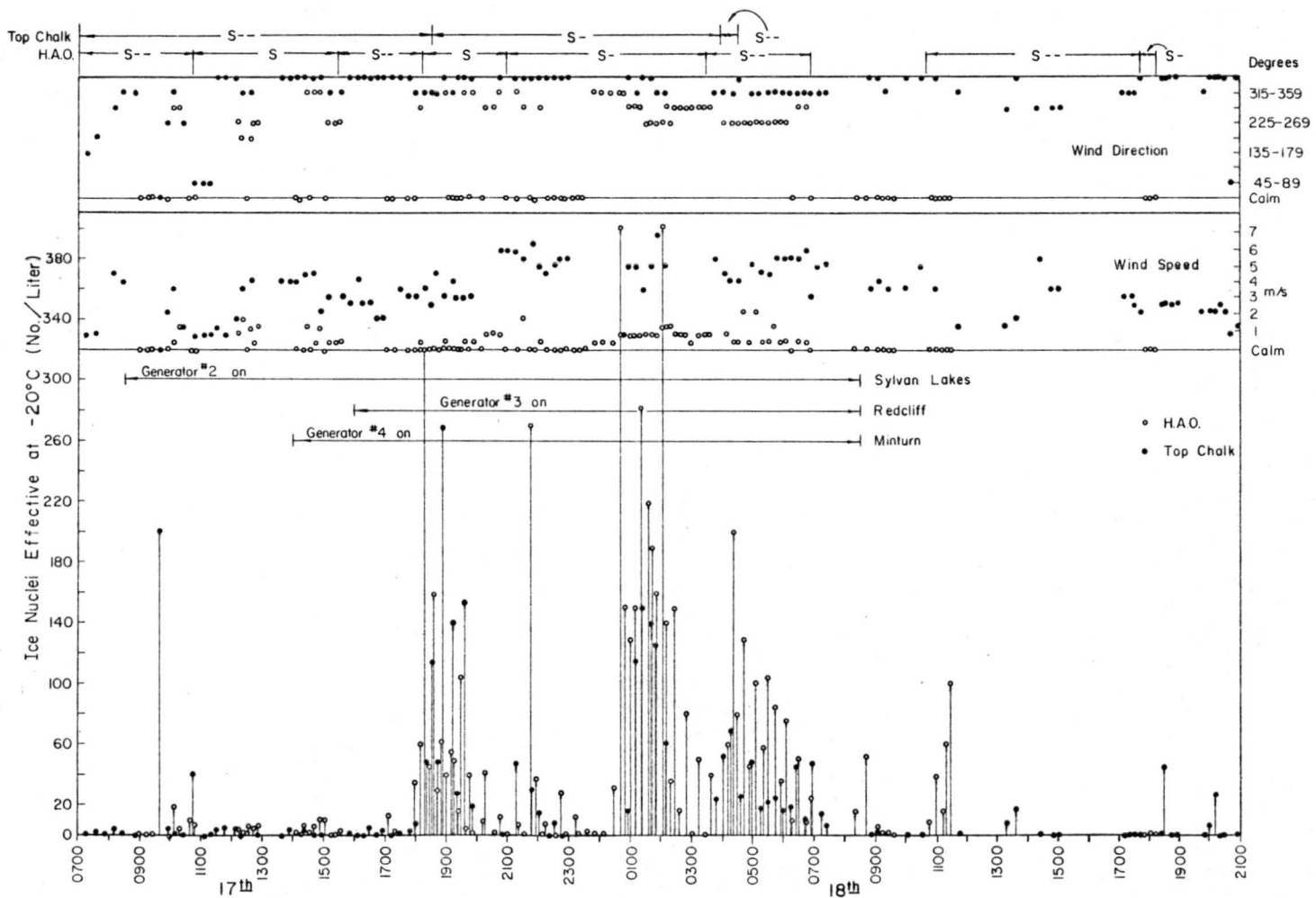


Figure 12 Change in ice nuclei concentration at Climax after seeding at upwind ground sites during light and moderate snowfall